J|A|C|S ARTICLES

Published on Web 04/27/2010

NMR Analyses of the Interaction between CCR5 and Its Ligand Using Functional Reconstitution of CCR5 in Lipid Bilayers

Chie Yoshiura,[†] Yutaka Kofuku,[†] Takumi Ueda,[†] Yoko Mase,[†] Mariko Yokogawa,[†] Masanori Osawa,[†] Yuya Terashima,[‡,§] Kouji Matsushima,[‡] and Ichio Shimada*[,†,||]

Graduate School of Pharmaceutical Sciences, The University of Tokyo, Hongo 7-3-1, Bunkyo-ku, Tokyo 113-0033, Japan, Department of Molecular Preventive Medicine, Graduate School of Medicine, The University of Tokyo, Hongo 7-3-1, Bunkyo-ku, Tokyo 113-0033, Japan, Effector Cell Institute, Inc., Tokyo 150-0036, Japan, and Biomedicinal Information Research Center (BIRC), National Institute of Advanced Industrial Science and Technology (AIST), Aomi 2-41-6, Koto-ku, Tokyo 135-0064, Japan

Received January 29, 2010; E-mail: shimada@iw-nmr.f.u-tokyo.ac.jp

Abstract: CC-chemokine receptor 5 (CCR5) belongs to the G protein-coupled receptor (GPCR) family and plays important roles in the inflammatory response. In addition, its ligands inhibit the HIV infection. Structural analyses of CCR5 have been hampered by its instability in the detergent-solubilized form. Here, CCR5 was reconstituted into high density lipoprotein (rHDL), which enabled CCR5 to maintain its functions for >24 h and to be suitable for structural analyses. By applying the methyl-directed transferred cross-saturation (TCS) method to the complex between rHDL-reconstituted CCR5 and its ligand MIP-1α, we demonstrated that valine 59 and valine 63 of MIP-1α are in close proximity to CCR5 in the complex. Furthermore, these results suggest that the protective influence on HIV-1 infection of a SNP of MIP-1α is due to its change of affinity for CCR5. This method will be useful for investigating the various and complex signaling mediated by GPCR, and will also provide structural information about the interactions of other GPCRs with lipids, ligands, G-proteins, and effector molecules.

Introduction

G-protein-coupled receptors (GPCRs), the largest family of integral membrane proteins, are remarkably versatile signaling molecules that recognize a wide variety of extracellular ligands, leading to the activation of intracellular coupling G proteins. Understanding the detailed mechanism of GPCR signaling is important, because many GPCRs are considered as the primary drug targets for various medical and pharmacological inventions.[1−3]

CC-chemokine receptor 5 (CCR5) is one of the members of the GPCR family. The interactions between CCR5 and its chemokines induce chemotactic responses in CCR5-expressing leukocytes.[4] CCR5 is reportedly the major coreceptor for HIV-1, and its ligands are potent inhibitors of HIV infection.[5−7] Several chemokines have been identified as the ligands of CCR5, including MIP-1α, MIP-1β, and RANTES.[8] Such promiscuity may allow the fine-tuning of the immune responses,[9] although the detailed mechanism of this phenomenon is still unclear. Therefore, the interactions between CCR5 and its ligands should be structurally clarified for understanding chemokine signaling.

Recently, several high-resolution structures of GPCRs have been solved: rhodopsin, β_2 adrenergic, β_1 adrenergic, A_2A adenosine, and the ligand-free form of rhodopsin (opsin).[10−20] These structures have provided important information for

[†] Graduate School of Pharmaceutical Sciences, The University of Tokyo.
[‡] Department of Molecular Preventive Medicine, Graduate School of Medicine, The University of Tokyo.
[§] Effector Cell Institute, Inc.
[||] Biomedicinal Information Research Center (BIRC).

(1) Deupi, X.; Kobilka, B. *Adv. Protein Chem.* **2007**, *74*, 137–66.
(2) Heilker, R.; Wolff, M.; Tautermann, C. S.; Bieler, M. *Drug. Discovery Today* **2009**, *14*, 231–40.
(3) Alkhalfioui, F.; Magnin, T.; Wagner, R. *Curr. Opin. Pharmacol.* **2009**, *9*, 629–35.
(4) Rajagopalan, L.; Rajarathnam, K. *Biosci. Rep.* **2006**, *26*, 325–39.
(5) Berger, E. A.; Murphy, P. M.; Farber, J. M. *Annu. Rev. Immunol.* **1999**, *17*, 657–700.
(6) Kuhmann, S. E.; Hartley, O. *Annu. Rev. Pharmacol. Toxicol.* **2008**, *48*, 425–61.
(7) Horuk, R. *Nat. Rev. Drug Discovery* **2009**, *8*, 23–33.
(8) Blanpain, C.; Migeotte, I.; Lee, B.; Vakili, J.; Doranz, B. J.; Govaerts, C.; Vassart, G.; Doms, R. W.; Parmentier, M. *Blood* **1999**, *94*, 1899–905.
(9) Allen, S. J.; Crown, S. E.; Handel, T. M. *Annu. Rev. Immunol.* **2007**, *25*, 787–820.
(10) Palczewski, K.; Kumasaka, T.; Hori, T.; Behnke, C. A.; Motoshima, H.; Fox, B. A.; Le Trong, I.; Teller, D. C.; Okada, T.; Stenkamp, R. E.; Yamamoto, M.; Miyano, M. *Science* **2000**, *289*, 739–45.
(11) Okada, T.; Sugihara, M.; Bondar, A. N.; Elstner, M.; Entel, P.; Buss, V. *J. Mol. Biol.* **2004**, *342*, 571–83.
(12) Cherezov, V.; Rosenbaum, D. M.; Hanson, M. A.; Rasmussen, S. G.; Thian, F. S.; Kobilka, T. S.; Choi, H. J.; Kuhn, P.; Weis, W. I.; Kobilka, B. K.; Stevens, R. C. *Science* **2007**, *318*, 1258–65.
(13) Rasmussen, S. G.; Choi, H. J.; Rosenbaum, D. M.; Kobilka, T. S.; Thian, F. S.; Edwards, P. C.; Burghammer, M.; Ratnala, V. R.; Sanishvili, R.; Fischetti, R. F.; Schertler, G. F.; Weis, W. I.; Kobilka, B. K. *Nature* **2007**, *450*, 383–7.
(14) Rosenbaum, D. M.; Cherezov, V.; Hanson, M. A.; Rasmussen, S. G.; Thian, F. S.; Kobilka, T. S.; Choi, H. J.; Yao, X. J.; Weis, W. I.; Stevens, R. C.; Kobilka, B. K. *Science* **2007**, *318*, 1266–73.
(15) Hanson, M. A.; Cherezov, V.; Griffith, M. T.; Roth, C. B.; Jaakola, V. P.; Chien, E. Y.; Velasquez, J.; Kuhn, P.; Stevens, R. C. *Structure* **2008**, *16*, 897–905.

 10.1021/ja100830f

understanding how GPCRs work at a molecular level. However, little is known about the structures of the active GPCRs bound to agonists or the dynamics that regulate the GPCR activity.

We recently applied the methyl-directed transferred cross-saturation (TCS) method to analyze the interaction between the detergent-solubilized chemokine receptor CXCR4 and its ligand chemokine SDF-1, and determined the contact surface on the SDF-1 molecule.[21] However, this methodology was not directly applicable for CCR5, because CCR5 in detergent micelles was much less stable than CXCR4 (see below).

It is generally accepted that membrane proteins maintain their native conformation more stably in lipid bilayers than in detergent micelles. Several membrane protein-reconstitution techniques were reported, such as bicelles, liposomes, and bead-linked proteoliposome.[22−24] Recently, a novel method for reconstituting active membrane proteins into nanoscale particles composed of phospholipid bilayers has been reported. These particles are referred to as nanodiscs, nanolipoprotein particles (NLPs), or reconstituted high density lipoprotein (rHDL).[25,26] rHDL is composed of phospholipid bilayers, containing embedded membrane proteins, and a dimer of apolipoprotein A-I (Apo A-I), which stabilizes the discoidal bilayer and controls its size. rHDL has reportedly been used in atomic force microscopy, electron microscopy, solid state NMR, and biochemical analyses. In addition, rHDL is a promising method for solution NMR studies, because of its water solubility and monodisperse character. The application of rHDL-embedded proteins to solution NMR has so far been limited to a membrane active peptide, a single-pass transmembrane peptide, and a multipass transmembrane protein, which retained the ligand binding activity in the detergent-solubilized form during the NMR measurements, though.[27−29]

Here, we successfully incorporated CCR5, which is very labile in the detergent micelles, into rHDL, and investigated the interaction between CCR5 and MIP-1α. The stability of CCR5 embedded in rHDL (CCR5−rHDL) was sufficient for solution NMR analyses. CCR5 in rHDL exhibited the signal transduction activity in a GDP−GTP exchange assay. In addition, we developed MIP-1α variants that are monodisperse at neutral pH, while retaining the binding activity to CCR5. We performed methyl-directed transferred cross-saturation (TCS) experiments, and identified the MIP-1α residues that are in close proximity to CCR5 embedded in rHDL. The methods established here will be applicable to various GPCRs in the active state.

Materials and Methods

Reagents. All reagents were from Nacalai Tesque and Wako Chemicals, unless otherwise noted.

Preparation of MIP-1α, MIP-1*β*, and Their Variants. The full-length cDNAs encoding MIP-1α and MIP-1*β* were cloned and amplified from a human cDNA library by PCR, with NdeI and BamHI sites at the 5′- and 3′-ends, respectively. The cDNAs encoding MIP-1α and MIP-1*β* were inserted into the pET19b vector (Novagen) containing an N-terminal His10 tag and an enterokinase cleavage site. The Nde I site was eliminated by using pairs of complementary primers and a QuikChange site-directed mutagenesis kit (Stratagene). The gene encoding the MIP-1α variant (P8A/F13Y/E67Q) was prepared using the QuikChange procedure.

The MIP-1α and MIP-1*β* expression plasmids were transformed into *Escherichia coli* strain BL21 Origami B (DE3) (Novagen). Cells were grown at 37 °C in 40 mL of Luria−Bertani (LB) medium for 12 h, and were then harvested and resuspended in fresh M9 minimal medium. Uniformly ^{13}C- and ^{15}N-labeled proteins for spectral assignments were produced in M9 minimal medium with 1 g/L $^{15}NH_4Cl$ (99.9% isotope enrichment) and 2 g/L [$^{13}C_6$]-glucose (98% isotope enrichment). For methyl-TCS experiments, the [u-^{2}H, (Ileδ1-, Leu-, Val-$^{13}C^1H_3$)] labeled protein was produced in 99.8% ^2H_2O M9 minimal medium with 2 g/L [$^2H_7$]-glucose, and with 50 mg/L [4-^{13}C, 3, 3-d_2]-α-ketobutyrate (CIL) and 120 mg/L [dimethyl-$^{13}C_2$]-α-ketoisovalerate (CIL, deuteration at position 3 was achieved by an incubation in ^2H_2O, pH 12.5, at 45 °C for 3 h) 30 min prior to induction.[30] Protein expression was induced by the addition of isopropyl-*β*-D-thiogalactopyranoside (IPTG) to a final concentration of 0.1 mM when the culture reached an OD_{600} of 0.7−0.9. After shaking incubation at 25 °C for 20 h, the cells were pelleted by centrifugation at 7000*g* for 10 min. The purification of MIP-1α and MIP-1*β* was performed as described previously.[31]

Preparation of the Apolipoprotein A-I Variant (N-Terminally His-Tagged MSPE3). The cDNA encoding apolipoprotein A-I (44−243) was amplified from a human liver cDNA library (Takara), and was inserted into the pET19b vector at the NdeI−BamHI sites. The sequence of Apo A-I (44−163) was further amplified from the pET19b-Apo A-I plasmid by PCR, with an NdeI site at the 5′ end and a SacII site at the sequence encoding H162-A164. A SacII restriction site was introduced into the pET19b-Apo A-I plasmid by site-directed mutagenesis at the sequence encoding Lys96. The pET19b-Apo A-I plasmid with the SacII site was digested with NdeI and SacII, and the amplified Apo A-I (44−163) fragment was inserted. During the construction process, the H162A/L163 V/A164Q mutations were introduced in the obtained MSPE3 gene. Hereafter, we refer to the gene as MSPE3. The gene encoding MSPE3 containing a C-terminal 1D4-tag (MSPE3-1D4) was prepared by inserting the gene encoding 1D4 tag just before the stop codon of the MSPE3 gene by the QuikChange site-directed mutagenesis.

MSPE3 was produced in *E. coli* strain BL21 (DE3) Codon-PlusRP, grown in 1 L of LB medium. Protein expression was induced by the addition of IPTG to a final concentration of 1 mM when the culture reached an OD_{600} of 1.0. After shaking incubation

(16) Jaakola, V. P.; Griffith, M. T.; Hanson, M. A.; Cherezov, V.; Chien, E. Y.; Lane, J. R.; Ijzerman, A. P.; Stevens, R. C. *Science* **2008**, *322*, 1211–7.
(17) Park, J. H.; Scheerer, P.; Hofmann, K. P.; Choe, H. W.; Ernst, O. P. *Nature* **2008**, *454*, 183–7.
(18) Scheerer, P.; Park, J. H.; Hildebrand, P. W.; Kim, Y. J.; Krauss, N.; Choe, H. W.; Hofmann, K. P.; Ernst, O. P. *Nature* **2008**, *455*, 497–502.
(19) Warne, T.; Serrano-Vega, M. J.; Baker, J. G.; Moukhametzianov, R.; Edwards, P. C.; Henderson, R.; Leslie, A. G.; Tate, C. G.; Schertler, G. F. *Nature* **2008**, *454*, 486–91.
(20) Hanson, M. A.; Stevens, R. C. *Structure* **2009**, *17*, 8–14.
(21) Kofuku, Y.; Yoshiura, C.; Ueda, T.; Terasawa, H.; Hirai, T.; Tominaga, S.; Hirose, M.; Maeda, Y.; Takahashi, H.; Terashima, Y.; Matsushima, K.; Shimada, I. *J. Biol. Chem.* **2009**, *284*, 35240–50.
(22) Diller, A.; Loudet, C.; Aussenac, F.; Raffard, G.; Fournier, S.; Laguerre, M.; Grelard, A.; Opella, S. J.; Marassi, F. M.; Dufourc, E. J. *Biochimie* **2009**, *91*, 744–51.
(23) Rigaud, J. L.; Levy, D. *Methods Enzymol.* **2003**, *372*, 65–86.
(24) Yokogawa, M.; Takeuchi, K.; Shimada, I. *J. Am. Chem. Soc.* **2005**, *127*, 12021–7.
(25) Nath, A.; Atkins, W. M.; Sligar, S. G. *Biochemistry* **2007**, *46*, 2059–69.
(26) Borch, J.; Hamann, T. *Biol. Chem.* **2009**, *390*, 805–14.
(27) Raschle, T.; Hiller, S.; Yu, T. Y.; Rice, A. J.; Walz, T.; Wagner, G. *J. Am. Chem. Soc.* **2009**, *131* (49), 17777–9.
(28) Gluck, J. M.; Wittlich, M.; Feuerstein, S.; Hoffmann, S.; Willbold, D.; Koenig, B. W. *J. Am. Chem. Soc.* **2009**, *131*, 12060–1.
(29) Shenkarev, Z. O.; Lyukmanova, E. N.; Solozhenkin, O. I.; Gagnidze, I. E.; Nekrasova, O. V.; Chupin, V. V.; Tagaev, A. A.; Yakimenko, Z. A.; Ovchinnikova, T. V.; Kirpichnikov, M. P.; Arseniev, A. S. *Biochemistry (Moscow)* **2009**, *74*, 756–65.
(30) Goto, N. K.; Gardner, K. H.; Mueller, G. A.; Willis, R. C.; Kay, L. E. *J. Biomol. NMR* **1999**, *13*, 369–74.
(31) Sugiki, T.; Yoshiura, C.; Kofuku, Y.; Ueda, T.; Shimada, I.; Takahashi, H. *Protein Sci.* **2009**, *18*, 1115–20.

at 30 °C for 6 h, the cells were collected by centrifugation. The cells were lysed by sonication in the presence of 1% Triton X-100. The lysate was purified by Ni affinity chromatography, as previously described,[32] the imidazole was removed from the elution fraction by dialysis, and the purified protein was stored in buffer containing 20% glycerol.

Control rHDL was prepared from MSPE3 and POPC, as previously described.[32] rHDL composed of the lipids derived from Sf9 cells was also prepared with the solubilized cell membranes by 1% *n*-dodecyl-β-D-maltopyranoside (DDM). In size exclusion chromatography analyses, the retention time of rHDL was almost identical to that in the previous report; thus, the size of rHDL used in the present study is similar to that prepared from MSPE3 in previous report (Supporting Information Figure S1).

Preparation of the CCR5 Construct for the Insect Expression System. The cDNA fragment encoding human CCR5 was amplified by PCR, and was cloned into the pBac6 vector (Novagen) at the NcoI−BamHI sites. A fragment encoding 10 linker residues and the C-terminal 14 residues (TTVSKTETSQVAPA) of bovine rhodopsin was introduced just before the stop codon of the CCR5 gene, as a 1D4 antibody epitope tag (1D4-tag). We named this plasmid pBac6-CCR5-1D4.

Sf9 cells (Invitrogen) were routinely maintained at 27 °C in Grace's supplemented medium (GIBCO), containing 10% fetal bovine serum (Biowest), 0.1% Pluronic F-68 (GIBCO), 50 international units/mL penicillin, 50 μg/mL streptomycin, and 0.125 μg/mL amphotericin B. Recombinant baculoviruses were generated using the BacVector Transfection kit (Novagen) according to the manufacturer's instructions. Briefly, pBac6-CCR5-1D4 was co-transfected with the BacVector-1000 Triple Cut Virus DNA into Sf9 cells to produce CCR5 viruses. Recombinant viruses were plaque-purified and amplified to generate high-titer virus stocks.

Expression of CCR5 and Preparation of the CCR5-Containing Membranes. For large-scale expression, a 0.4 L culture of Sf9 cells was grown in a 1-L spinner flask (Bellco). The Sf9 cells were inoculated at a density of 2×10^6 cells/mL with the high-titer virus stock (20 mL per 0.4 L of cells), and with 5 μg/mL of the cysteine protease inhibitor E64 (Peptide Institute, Inc.). Cells were harvested by centrifugation at 2000*g* at 36 h post infection. The resulting cell pellets were stored at −80 °C.

For the preparation of the membrane fraction, CCR5-expressing Sf9 cells were lysed by sonication in a buffer (50 mM Tris, 1 mM EDTA, pH 7.5) containing 30% sucrose, as part of a discontinuous sucrose density gradient (60%, 30%, and 5%). After ultracentrifugation at 45 000 rpm and 4 °C for 6 h with a 70 Ti rotor and an Optima L-90K centrifuge (Beckman), the membrane fraction was recovered from the 5−30% parts. This fraction was diluted by the buffer without sucrose and was further processed by centrifugation (10 000*g* for 1 h in a Beckman JA 30.50 rotor). The pellet was collected and resuspended in buffer containing 20% glycerol.

Preparation of CCR5−rHDL. The CCR5-containing membrane fraction, prepared from a 1.6 L culture of Sf9 cells, was solubilized with 10 mL of HBSG buffer (20 mM Hepes, 150 mM NaCl, 20% glycerol, pH 7.8) containing 1% DDM and a protease inhibitor cocktail (Nacalai Tesque). After a 40 min incubation at 4 °C, MSPE3 (30 mg) was added to achieve a final concentration of 50 μM. The final volume of the reconstitution mixture was about 20 mL. The reconstitution mixture was incubated for 15 min at 4 °C, and the self-assembly process was initiated by removing DDM by adding 2.5 g of Bio-Beads SM-2 (Bio-Rad). The mixture was incubated with the beads for 1 h at 4 °C with gentle agitation, and the beads were removed. This process was repeated twice.

The reconstitution mixture was loaded onto a Ni-affinity chromatography column (5 mL) equilibrated with the HBSG buffer. The column was washed with 30 mL of HBSG containing 10 mM imidazole, and the rHDL was eluted with 10 mL of HBSG containing 200 mM imidazole.

The fraction containing CCR5−rHDL was mixed with 0.5 mL of 1D4-Sepharose, in which 3.5 mg/mL of the 1D4 antibody (University of British Columbia) was coupled with CNBr-activated Sepharose 4B (GE Healthcare). The mixture was incubated for 3 h at 4 °C, and the supernatant was removed after centrifugation. The beads were washed three times with 10 mL of HBSG. The purified CCR5−rHDL was eluted with buffer (for the TCS experiment: 20 mM Hepes, 100 mM NaCl, 5% (v/v) glycerol-d_8, 95% D_2O) containing 0.4 mg/mL of the nonapeptide TETSQVAPA (1D4-peptide, synthesized by Toray Research Center). The elution buffer was mixed with the beads and incubated overnight, and the supernatant including CCR5−rHDL was collected by centrifugation.

The yield and purity of the prepared CCR5−rHDL were analyzed by SDS−PAGE and native-PAGE. SDS−PAGE was performed on 10−12% gradient acrylamide gels (ATTO Corporation). Native-PAGE was performed on 4−20% gradient acrylamide gels in Tris-glycine (Invitrogen). Gels were stained with a Silver Staining Kit (Daiichi Pure Chemicals) or were subjected to Western blotting with 1D4 antibody.

For the analysis of MIP-1β binding activity, the CCR5−rHDL was combined with an excess amount of MIP-1β (final 2 μM) and 100 μL of 1D4-Sepharose, and was incubated at 4 °C for 2 h. To remove the unbound MIP-1β, the mixture was centrifuged, and the beads were washed three times with HBSG. A 200 μL aliquot of 0.4 mg/mL 1D4-peptide in HBSG was added to the washed beads and incubated overnight. All fractions were analyzed by SDS−PAGE on a 4−20% gradient gel and silver staining.

SPR Analysis. The 2D7 binding activities of CCR5 were analyzed by SPR measurements using a BIAcore 2000 instrument (Biacore) as described previously[33] with minor modifications. Briefly, 1D4 antibodies were immobilized on the sensor chip CM5 using standard amine-coupling chemistry, resulting in a signal of 12 000−15 000 resonance units. The binding assay was performed in running buffer (20 mM Hepes, pH 7.2, 100 mM NaCl, with or without 0.1% DDM) at a flow rate of 20 μL/min. In each analysis cycle, CCR5 was first captured on the sensor chip via 1D4 antibodies, and then a 10 min washing step was performed with the running buffer. Antibody binding was observed by an injection of 1.2 ng of 2D7 antibodies (Pharmingen) for 2 min. The bound receptors were removed from the chip surface by microinjections of 10 mM NaOH + 1% *n*-octyl-β-D-glucoside (Dojindo). The sensorgrams were processed using the BIAevaluation 3.0 software (Biacore).

For the analysis of the stability of CCR5 in detergent micelles, CCR5-expressing Sf9 membranes, obtained from 10 mL of Sf9 culture, were solubilized in 0.5 mL of running buffer containing 1% DDM. After a 40 min incubation at 4 °C, the supernatant was collected by centrifugation. A 120 μL aliquot of the solubilized CCR5 was injected for analysis in the running buffer with 0.1% DDM.

The analysis of CCR5−rHDL was carried out using the running buffer without DDM.

The MIP-1α variant binding activity of CCR5−rHDL was analyzed using a BIAcore T−100 instrument (Biacore). CCR5−rHDL was captured on the sensor chip CM5. Empty-rHDL composed of the lipids derived from Sf9 cells and MSPE3-1D4 was captured on the control flow cell. The binding assay was performed in running buffer (20 mM Hepes, pH 7.2, 100 mM NaCl) at a flow rate of 30 μL/min, using serial dilutions of the MIP-1α variant in the 0.33−13.2 μM range. The dissociation constant was obtained from the steady-state curve fitting analysis, using Biacore T100 Evaluation Software (Biacore).

(32) Denisov, I. G.; Grinkova, Y. V.; Lazarides, A. A.; Sligar, S. G. *J. Am. Chem. Soc.* **2004**, *126*, 3477–87.

(33) Navratilova, I.; Sodroski, J.; Myszka, D. G. *Anal. Biochem.* **2005**, *339*, 271–81.

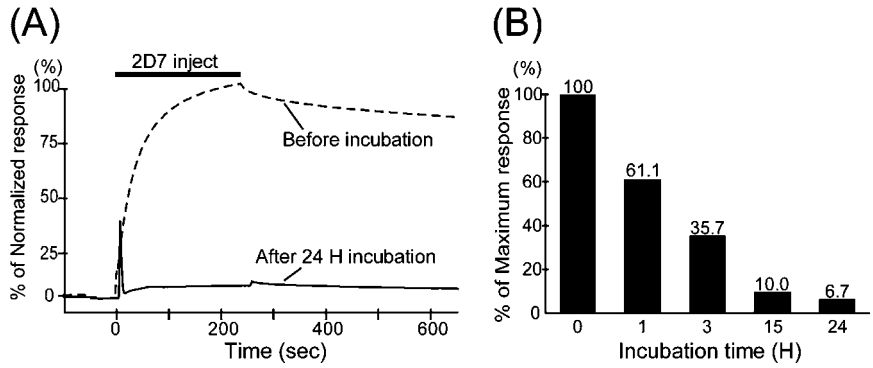

Figure 1. Stability of the solubilized CCR5. (A) Normalized SPR responses for 2D7 antibody binding to CCR5 in DDM micelles immediately after solubilization (dotted line) and after a 24 h incubation at 4 °C (solid line). Responses were normalized for the amount of the captured CCR5. (B) Decrease of receptor activity over time. The bars show the relative values of the responses for 2D7 antibody binding of CCR5 in DDM micelles (immediately after solubilization = 100%). The maximum RU values were obtained after the end of a 4-min association phase and were normalized for the amount of the captured CCR5.

Guanine Nucleotide Exchange Assay. The heterotrimeric G protein was prepared, according to the reports[34−37] with minor modifications. The human $G\alpha_{i3}$ subunit of the heterotrimeric G-protein, containing a C-terminal His10 tag, was expressed in *E. coli* and was purified by Ni affinity chromatography and anion exchange chromatography. The bovine $G\beta_1$ and human $G\gamma_2$ (C68S mutant) subunit was expressed in Sf9 cells with a His tag at the N-terminus of the $G\gamma$ subunit and was purified by Ni affinity chromatography.

The purified CCR5−rHDL was incubated with the G proteins and MIP-1β in a final volume of 0.3 mL of buffer (20 mM Hepes, pH 7.8, 150 mM NaCl, 10 mM $MgCl_2$, and 10 μM GDP). The reaction mixtures were incubated for 45 min at 4 °C with gentle agitation, and a 30 μL aliquot of nonhydrolyzable GTP modified with fluorescent Europium (Eu-GTP, PerkinElmer) was added to a final concentration of 10 nM. The reaction mixtures were further incubated for 30 min at 4 °C, and the reaction was terminated by the addition of nonlabeled GTPγS (PerkinElmer) to a final concentration of 5 μM. To capture the Gα subunit with its N-terminal His-tag, each mixture was combined with 100 μL of the equilibrated Ni affinity beads, and was diluted with buffer to a final volume of 0.9 mL. After a 2 h incubation, the beads were applied to three wells in an AcroWell filter plate (Pall). To remove the unbound Eu-GTP, the beads were washed twice by filtration through the filters with 0.3 mL of the HBSG buffer. The bound Eu-GTP was measured, using an Envision 2103 Multilabel Reader (PerkinElmer), with excitation at 320 nm and emission was measured at 620 nm.

NMR Experiments. NMR experiments of MIP-1α in the unbound form were carried out at 30 °C in 20 mM Hepes, pH 6.0, containing 100 mM NaCl, in H_2O/D_2O = 90/10 with Bruker Avance 500 or 600 spectrometers equipped with cryogenic probes.

$^1H-^{15}N$ HSQC spectra of MIP-1α were recorded using uniformly ^{15}N-labeled 50 μM MIP-1α variants. 1D TRACT spectra were recorded with Δ_i = 0.1, 10, 20, 30, 40 ms, and the effective rotational correlation time (τ_c) was calculated as described previously.[38] NMR spectral assignments were performed with 50 μM of the uniformly ^{13}C- and ^{15}N-labeled MIP-1α variants at pH 6.0. Sequential assignments of the backbone resonances were achieved by the sets of three-dimensional triple resonance experiments (HNCA, CBCA(CO)NH). Assignments of methyl resonances from isoleucine, leucine, and valine residues were achieved by $^1H-^{13}C$ ct-HSQC and (H)CCH-TOCSY experiments.[39,40]

In the methyl-TCS experiments, a 10 μM (final concentration) of lyophilized [u-^2H, (Ile-, Leu-, Val-$^{13}C^1H_3$)]-MIP-1α variants were combined with about 1/10 mol equiv of CCR5−rHDL in 20 mM Hepes, pH 6.0, 100 mM NaCl, H_2O/D_2O = 1/99, 5% (v/v) glycerol-d_8. For negative control experiments, the same experiments mentioned above were performed with the sample including the rHDL composed of the lipids derived from Sf9 cells. All of the methyl-TCS spectra were recorded at 10 °C with a Bruker Avance 800 spectrometer equipped with a cryogenic probe, using the pulse scheme as described previously.[41] The irradiation frequency was set at 6.5 ppm, and the maximum radiofrequency amplitude was 0.21 kHz for WURST-20 (the adiabatic factor Q_0 = 1).[42] The irradiation time and the additional relaxation times were set to 1.0 and 4.0 s, respectively.

The recorded spectra were processed by XWIN-NMR (Bruker) or Topspin 2.0 (Bruker), and were analyzed by Sparky.[43]

Results

Evaluation of CCR5 Stability in DDM Micelles. CCR5 with a C-terminal 1D4 epitope-tag was expressed in Sf9-insect cells, using the baculovirus expression system.[44,45] CCR5 embedded in the cell membranes was solubilized by 1% DDM and used in following analyses. To examine the conformational integrity of CCR5 expressed in Sf9-insect cells, the binding activity with the conformation dependent anti-CCR5 antibody 2D7, which recognizes ECL2 of CCR5 in its native conformation,[46,47] was

(34) Iniguez-Lluhi, J. A.; Simon, M. I.; Robishaw, J. D.; Gilman, A. G. *J. Biol. Chem.* **1992**, *267*, 23409–17.
(35) Kozasa, T.; Gilman, A. G. *J. Biol. Chem.* **1995**, *270*, 1734–41.
(36) Lee, E.; Linder, M. E.; Gilman, A. G. *Methods Enzymol.* **1994**, *237*, 146–64.
(37) Di Cesare Mannelli, L.; Pacini, A.; Toscano, A.; Fortini, M.; Berti, D.; Ghelardini, C.; Galeotti, N.; Baglioni, P.; Bartolini, A. *Protein Expression Purif.* **2006**, *47*, 303–10.
(38) Lee, D.; Hilty, C.; Wider, G.; Wuthrich, K. *J. Magn. Reson.* **2006**, *178*, 72–6.
(39) Clore, G. M.; Gronenborn, A. M. *Methods Enzymol.* **1994**, *239*, 349–63.
(40) Senn, H.; Wernera, B.; Messerlea, B. A.; Webera, C.; Traberb, R.; Wuthrich, K. *FEBS Lett.* **1989**, *249*, 113–118.
(41) Takahashi, H.; Miyazawa, M.; Ina, Y.; Fukunishi, Y.; Mizukoshi, Y.; Nakamura, H.; Shimada, I. *J. Biomol. NMR* **2006**, *34*, 167–77.
(42) Kupce, E.; Wagner, G. *J. Magn. Reson. B* **1995**, *109*, 329–333.
(43) Goddard, T. D.; Kneller, D. G. *SPARKY 3*, University of California: San Francisco, CA, 2006.
(44) McCusker, E. C.; Bane, S. E.; O'Malley, M. A.; Robinson, A. S. *Biotechnol. Prog.* **2007**, *23*, 540–7.
(45) Sarramegn, V.; Muller, I.; Milon, A.; Talmont, F. *Cell. Mol. Life Sci.* **2006**, *63*, 1149–64.
(46) Paes, C.; Ingalls, J.; Kampani, K.; Sulli, C.; Kakkar, E.; Murray, M.; Kotelnikov, V.; Greene, T. A.; Rucker, J. B.; Doranz, B. J. *J. Am. Chem. Soc.* **2009**, *131*, 6952–4.
(47) Lee, B.; Sharron, M.; Blanpain, C.; Doranz, B. J.; Vakili, J.; Setoh, P.; Berg, E.; Liu, G.; Guy, H. R.; Durell, S. R.; Parmentier, M.; Chang, C. N.; Price, K.; Tsang, M.; Doms, R. W. *J. Biol. Chem.* **1999**, *274*, 9617–26.

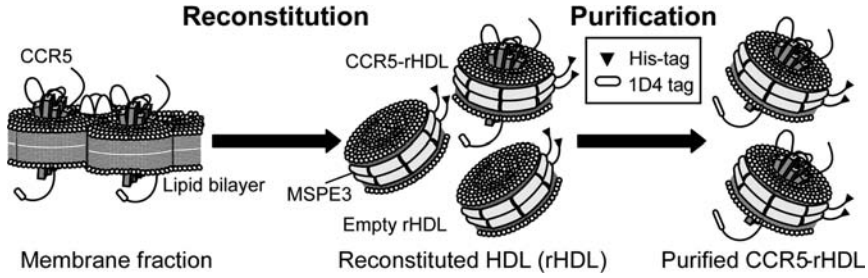

Figure 2. Schematic representation of the preparation of CCR5−rHDL. CCR5, embedded in Sf9 cell membranes was solubilized, immediately reconstituted into rHDL, and subsequently purified using the His-tag and the 1D4 tag in MSPE3 and CCR5, respectively.

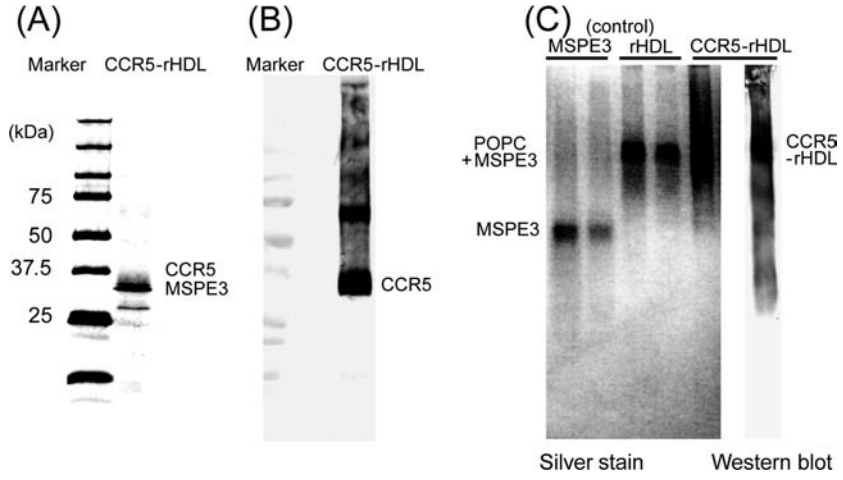

Figure 3. Characterization of CCR5−rHDL. (A and B) SDS−PAGE analysis of CCR5−rHDL. A 10 μL (A) or 5 μL (B) portion of 1 mL of purified CCR5−rHDL, prepared from a 1.6 L Sf9 culture, was loaded on a 10−20% gradient gel. In panels A and B, the gel was silver-stained and analyzed by Western blotting using the 1D4 antibody against the C-terminal 1D4 epitope-tag, respectively. Both CCR5 and MSPE3 migrated at ∼35 kDa. (C) Native-PAGE analysis of CCR5−rHDL. Purified CCR5−rHDL was loaded on a 4−20% gradient Tris-glycine native-PAGE gel. The gel was silver-stained or analyzed by Western blotting using the 1D4 antibody.

analyzed by SPR experiments[33,48,49] (Figure 1A, dotted line). The response was observed upon the addition of the 2D7-antibody to the sensor chip with freshly prepared CCR5. The expression conditions, such as the selection of promoters, MOI, and the addition of protease inhibitors, were optimized, using the conformation dependent 2D7 antibody binding activity obtained by SPR experiments. The expression level of CCR5 in the plasma membrane was about 0.5 nmol/L culture, as judged from Western blotting with the 1D4 antibody.

To examine the stability of CCR5 in DDM micelles, we analyzed the time course of the 2D7-antibody binding activity. As a result, the response of 2D7 for CCR5 immobilized on the sensor chip was reduced to 50% after a 3 h incubation at 4 °C (Figure 1B), and was undetectable after a 24 h incubation (Figure 1A, solid line), even though DDM, which is a suitable detergent for the solubilization of CCR5,[33,48,49] was used in the experiment.

Reconstitution of CCR5 into rHDL. For the preparation of functional CCR5, we employed the rHDL system for lipid bilayer reconstitution, as follows (Figure 2). The plasma membrane of the Sf9 cells was partially purified by sucrose gradient ultracentrifugation to remove the soluble impurities. CCR5 was solubilized by DDM and then immediately reconstituted into rHDL, using MSPE3 with the N-terminal His tag.[32] CCR5 in rHDL (CCR5−rHDL) was purified by removing the nonreconstituted elements, using Ni affinity chromatography, and then subsequently removing the rHDL without CCR5, using 1D4 antibody affinity chromatography, which has high efficiency and specificity for the 1D4 tag of CCR5.[50] The purity of CCR5−rHDL was ∼80%, as judged from the SDS−PAGE pattern (Figure 3A). An additional minor band with a higher mobility (∼25 kDa) was not stained with the Western blotting analysis with the 1D4-antibody. The Western blotting was carried out immediately after the 1D4 affinity chromatography purification, indicating that all CCR5 molecules in the sample must contain the C-terminal 1D4 tag. In contrast, the Western blotting analysis revealed that the minor band does not contain the C-terminal 1D4 tag Therefore, we concluded that the minor band is not derived from the N-terminal truncated CCR5, but probably from the partially truncated MSPE3. The Western-blotting analyses with the 1D4 antibody revealed that about 10 μg (∼ 0.25 nmol) of CCR5 reconstituted in rHDL were obtained from a 1 L Sf9 culture (Figure 3B). In the native PAGE analyses (Figure 3C), the particle size of CCR5−rHDL was same as that of rHDL prepared with POPC, suggesting that CCR5 was correctly reconstituted into rHDL.[32]

The conformational integrity of CCR5 reconstituted in rHDL was examined by the SPR experiment, using the conformation dependent 2D7 antibody (Figure 4, dotted line). The response

(48) Navratilova, I.; Pancera, M.; Wyatt, R. T.; Myszka, D. G. *Anal. Biochem.* **2006**, *353*, 278–83.
(49) Rich, R. L.; Miles, A. R.; Gale, B. K.; Myszka, D. G. *Anal. Biochem.* **2009**, *386*, 98–104.
(50) Mirzabekov, T.; Bannert, N.; Farzan, M.; Hofmann, W.; Kolchinsky, P.; Wu, L.; Wyatt, R.; Sodroski, J. *J. Biol. Chem.* **1999**, *274*, 28745–50.

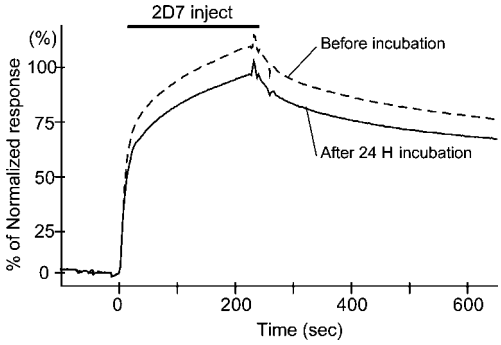

Figure 4. Normalized SPR responses for the binding of the 2D7 antibody to CCR5−rHDL immediately after preparation (dotted line) and after a 24 h incubation at 4 °C (solid line). Responses were normalized for the amount of the captured CCR5−rHDL.

of 2D7 to immobilized CCR5 was over 25% that of CCR5−rHDL to the sensor chip. These results suggest that at least 50% of CCR5 in rHDL should be correctly folded, because the estimated molecular mass of CCR5−rHDL is about twice of IgG antibodies.[51]

To examine the stability of CCR5−rHDL, we analyzed the time course of the binding activity to 2D7 by SPR (Figure 4). About 85% of the initial 2D7 antibody binding was retained after a 24 h incubation at 4 °C.

Characterization of the Biological Function of CCR5 Reconstituted into rHDL. The ECL2 of CCR5, which is recognized by the 2D7-antibody, assumed the active conformation. However, the binding of 2D7 does not necessarily mean that the other parts of CCR5 take the correct folding. Therefore, we examined the MIP-1β binding activities to CCR5−rHDL by pull-down assays. Substantial amounts of MIP-1β were coeluted with CCR5−rHDL upon addition of the 1D4 peptide, suggesting that the obtained CCR5−rHDL binds to MIP-1β (Figure 5A). It is likely that MIP-1β was under equilibrium between monomer and oligomer under the experimental condition with the concentration of 2 μM at pH 7.8, and that the monomer component binds to CCR5−rHDL. The reported dissociation constant of dimer MIP-1β to the monomer is 0.73 μM.[69] In addition, the estimated dissociation constants of CCR5−rHDL and wild-type MIP-1β are $\sim 10^{-7}$ M (Figure 5B, see below). These dissociation constants revealed that >80% of CCR5−rHDL can bind to MIP-1β under the condition described above. The coelution was also observed for MIP-1α (data not shown).

The binding of agonists to GPCRs stimulates the exchange of GDP for GTP in the Gα subunit of the coupling heterotrimeric G-proteins, which induces intracellular signal transduction. To examine whether CCR5 embedded in rHDL retains this biological activity, we performed a GDP−GTP exchange assay. The GDP−GTP exchange process on the Gα subunit was monitored by measuring the binding of nonhydrolyzable GTP modified with fluorescent europium (Eu-GTP).[52−55] The intensity of the fluorescence was increased, dependent on the concentration of wild-type MIP-1β, with a median effective concentration (EC_{50}) of about 100 nM (Figure 5B), suggesting that CCR5 embedded in rHDL was activated by MIP-1β and induced the GDP−GTP exchange on the Gα subunit. We carried out the control experiments with SDF-1, to examine whether the increase of the fluorescence in Figure 5B is specific to the physiological chemokine partners. The concentration-dependent increase of the fluorescence was not observed in the experiment with SDF-1, suggesting that the activation of the GDP−GTP exchange observed in the experiments with MIP-1β is specific to the interaction with the physiological partners.

Development of MIP-1α Monomeric Variants. Many chemokines form dimers at concentrations in the high nanomolar or low micromolar range, and the interactions between chemokines and glycosaminoglycans (GAGs) promote chemokine dimerization.[56,57] Furthermore, several chemokines have a strong tendency to aggregate at neutral pH.[31,58] On the other hand, chemokines are considered to act as monomers under biological conditions, because the variant of MIP-1β that forms a covalent dimer (A10C) reportedly neither binds nor activates CCR5.[56]

Therefore, to develop monomeric variants of MIP-1α, we introduced P8A/F13Y/E67Q mutations into MIP-1α. The P8A and F13Y mutations were introduced in the dimer interface of MIP-1α to prevent dimerization, and the E67Q mutation reportedly prevents aggregation at neutral pH.[58] In the following, we refer to the P8A/F13Y/E67Q variant of MIP-1α as the MIP-1α variant, unless otherwise described.

One-dimensional TRACT experiments demonstrated that, at a 50 μM concentration, the MIP-1α variant exists as a monomer at pH 6.0, whereas the wild-type MIP-1α aggregates at pH 6.0 and exists as a dimer at pH 2.5 (Table 1). The MIP-1α variant exhibited a well-dispersed $^{1}H-^{15}N$ HSQC spectrum at pH 6.0 (Supporting Information Figure S2A), and the $^{13}C_{\alpha}$ and $^{13}C_{\beta}$ chemical shifts suggested that the secondary structural elements within the MIP-1α variant are similar to those of the wild-type MIP-1α (data not shown). In the $^{1}H-^{15}N$ HSQC spectra of the wild-type and the MIP-1α variant under acidic conditions (Supporting Information Figure S2B,C), the residues that showed different chemical shifts were located at the dimer interface (T9, A10, C11), suggesting that the MIP-1α variant was correctly folded. In addition, we confirmed that the MIP-1α variant could stimulate the signaling of CCR5 reconstituted in rHDL in the GDP−GTP exchange assay (Supporting Information Figure S4). On the basis of the assay, we estimated that the dissociation constant of the MIP-1α variant to CCR5 is about $\sim 10^{-6}$ M. The estimated affinity is lower than the detection limit of the pull-down assay ($\sim 10^{-6}$ M);[59] thus, we applied SPR to examine the binding between the MIP-1α variant and CCR5−rHDL. As a result, the responses were observed upon the addition of the MIP-1α variant to CCR5−rHDL immobilized on the sensor chip, and the estimated dissociation constant was ~ 5 μM (Figure 6).

Methyl-Directed TCS Experiments. We performed the methyl-directed TCS experiments[21,41] with CCR5−rHDL and the MIP-1α variant. We prepared the [u-^{2}H/Leu, Val, Ileδ1-$^{13}CH_3$]-

(51) Lyukmanova, E. N.; Shenkarev, Z. O.; Paramonov, A. S.; Sobol, A. G.; Ovchinnikova, T. V.; Chupin, V. V.; Kirpichnikov, M. P.; Blommers, M. J.; Arseniev, A. S. *J. Am. Chem. Soc.* **2008**, *130*, 2140–1.
(52) Mueller, A.; Mahmoud, N. G.; Goedecke, M. C.; McKeating, J. A.; Strange, P. G. *Br. J. Pharmacol.* **2002**, *135*, 1033–43.
(53) Mueller, A.; Strange, P. G. *FEBS Lett.* **2004**, *570*, 126–32.
(54) Mueller, A.; Mahmoud, N. G.; Strange, P. G. *Biochem. Pharmacol.* **2006**, *72*, 739–48.
(55) Haworth, B.; Lin, H.; Fidock, M.; Dorr, P.; Strange, P. G. *Biochem. Pharmacol.* **2007**, *74*, 891–7.
(56) Jin, H.; Shen, X.; Baggett, B. R.; Kong, X.; LiWang, P. J. *J. Biol. Chem.* **2007**, *282*, 27976–83.
(57) McCornack, M. A.; Boren, D. M.; LiWang, P. J. *Biochemistry* **2004**, *43*, 10090–101.
(58) Czaplewski, L. G.; et al. *J. Biol. Chem.* **1999**, *274*, 16077–84.
(59) Urh, M.; Simpson, D.; Zhao, K. *Methods Enzymol.* **2009**, *463*, 417–38.

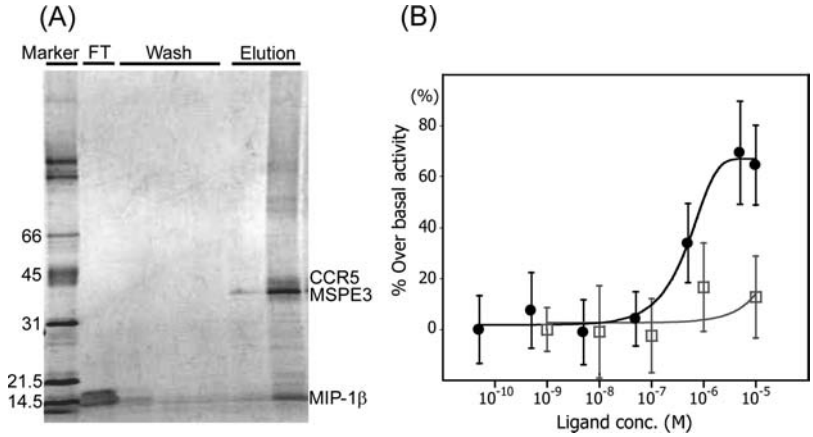

Figure 5. (A) MIP-1β binding activity of CCR5−rHDL, analyzed by a pull-down assay. Input: CCR5−rHDL bound to 1D4-Sepharose combined with excess amounts of wild-type MIP-1β. Flow through: the unbound fraction from the 1D4-Sepharose. Wash: the unbound MIP-1β was removed from the 1D4-Sepharose by three washes with HBSG buffer. Elution: the elution from the 1D4-Sepharose. Each fraction was loaded on a 4−20% gel, and the gel was silver-stained. CCR5−rHDL and MIP-1β migrated at ~35 kDa and ~14 kDa, respectively. (Both CCR5 and the Apo A-I variant migrated at 35 kDa.) (B) Eu-GTP binding to the complex of CCR5−rHDL and purified G protein, stimulated by wild-type MIP-1β. Eu-GTP binding was measured after an incubation in the presence of various concentrations of MIP-1β. Results are expressed as the percentage over the basal level of binding. Data represent the mean ± SE mean binding of triplicate determinations from a representative of three separate experiments. Circle and square symbols show the results of MIP-1β and SDF-1 as controls, respectively.

Table 1. Rotational Correlation Time (τ_c) and Estimated Molecular Mass of the MIP-1α Variants, Determined by 1D TRACT Experiments

MIP-1α	τ_c (ns)	estimated molecular mass (kDa)
Wild-type	12.7	27.5
P8A/F13Y/E67Q	5.6	12.2

labeled MIP-1α variant.[30] The hydrogens of the labeled MIP-1α variant, except for those of the methyl groups, were sufficiently deuterated for the methyl-directed TCS experiments (>98%, as judged from ^{1}H-1D NMR spectra). The methyl-TCS experiments were carried out with a sample containing 1 μM nonlabeled CCR5−rHDL and an excess amount (10 μM) of the labeled MIP-1α variant. In the methyl-TCS experiments, irradiation with a frequency corresponding to the methine and aromatic protons (4.5−8 ppm) was applied to the mixture of CCR5−rHDL and the labeled MIP-1α variant. The water-mediated proton relaxation of the large complexes[60] was not perturbed by the irradiation, because the experiments were carried out in D_2O. If the complex has an exchange rate between the free and bound states that is faster than the longitudinal relaxation rates of the methyl protons of the MIP-1α variant (1−2 s^{-1}), then the saturation in the proximal residues is sufficiently transferred to the free state of the MIP-1α variant. As a result, the proximal residues can be identified by the selective intensity reductions of the methyl resonances in the ^{1}H−^{13}C heteronuclear single quantum coherence (HSQC) spectrum of the unbound MIP-1α variant.

To selectively observe the specific interaction between CCR5−rHDL and the MIP-1α variant, we subtracted the nonspecific binding effects, such as interactions with lipids or the MSPE3 polypeptide, from the TCS results by the control experiments. In the control experiments, we used the rHDL without CCR5 (empty rHDL). For efficient saturation transfer for CCR5−rHDL, the exchange rate between the free and receptor-bound states of the MIP-1α variant must be sufficiently fast.[61−63] Considering the diffusion-controlled association rate constant (~10^6 M^{-1} s^{-1}) and the estimated dissociation constant of the MIP-1α variant to CCR5 (~5 μM), the exchange rate would be about 1−10 s^{-1}. The exchange sufficiently occurs during the irradiation time of 1 s. Therefore, TCS experiments are applicable under such conditions.[63] Our relaxation matrix calculations[41,63] revealed that the ligand methyl protons within 5 Å of the receptor's protons would exhibit intensity reductions of more than 0.1.

The difference in reduction ratios (ΔRRs), which represents the specific interaction between CCR5−rHDL and the MIP-1α variant, was calculated for each resonance, by subtracting the intensity reduction ratio in the control experiment using empty-rHDL from that in the TCS experiment. Supporting Information Figure S3 shows the ^{1}H−^{13}C HSQC spectrum of the MIP-1α variant observed in the TCS experiment. The ΔRRs were calculated for each resonance (Figure 7A,B), and the residues were colored according to their ΔRRs on the MIP-1α structure in the free state (Figure 7C). The methyl resonances derived from V59 and V63 exhibited high ΔRRs (>0.1).

To further eliminate the nonspecific binding effect between the ligands and the denatured CCR5, we performed another control experiment, in which the specific binding surface on the correctly folded CCR5 was selectively blocked by the addition of the stoichiometric amount of the nonlabeled conformation dependent 2D7 antibody (Supporting Information Figure S5). As a result, the resonances from V59 and V63 were not significantly affected by irradiation in the control experiment, and ΔRRs were less than 0.1, suggesting that the intensity reductions of these residues in Figure 7 are due to the specific interaction between properly folded CCR5−rHDL and the MIP-1α variant.

The spin diffusion effects and the effects of the residual protons in the MIP-1α variant should exert only minor effects,

(60) Riek, R.; Fiaux, J.; Bertelsen, E. B.; Horwich, A. L.; Wuthrich, K. *J. Am. Chem. Soc.* **2002**, *124*, 12144–53.
(61) Nakanishi, T.; Miyazawa, M.; Sakakura, M.; Terasawa, H.; Takahashi, H.; Shimada, I. *J. Mol. Biol.* **2002**, *318*, 245–9.
(62) Shimada, I. *Methods Enzymol.* **2005**, *394*, 483–506.
(63) Shimada, I.; Ueda, T.; Matsumoto, M.; Sakakura, M.; Osawa, M.; Takeuchi, K.; Nishida, N.; Takahashi, H. *Prog. Nucl. Magn. Reson. Spectrosc.* **2009**, *54*, 123–140.

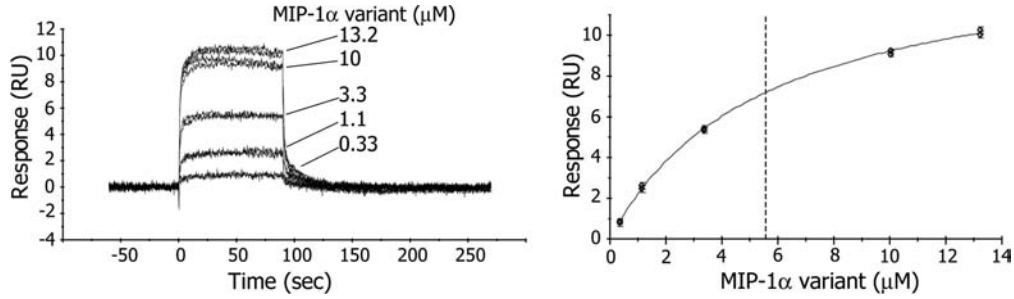

Figure 6. SPR analyses of the interaction between the MIP-1α variant and CCR5−rHDL. (A) Overlay plots of the sensorgrams obtained for the interaction between 0.33−13.2 μM of the MIP-1α variant and the immobilized CCR5−rHDL. The plots based on the steady-state method in SPR are shown in panel B. Each point is the average of 50 data points in the sensorgram, and the error bars are their standard deviations.

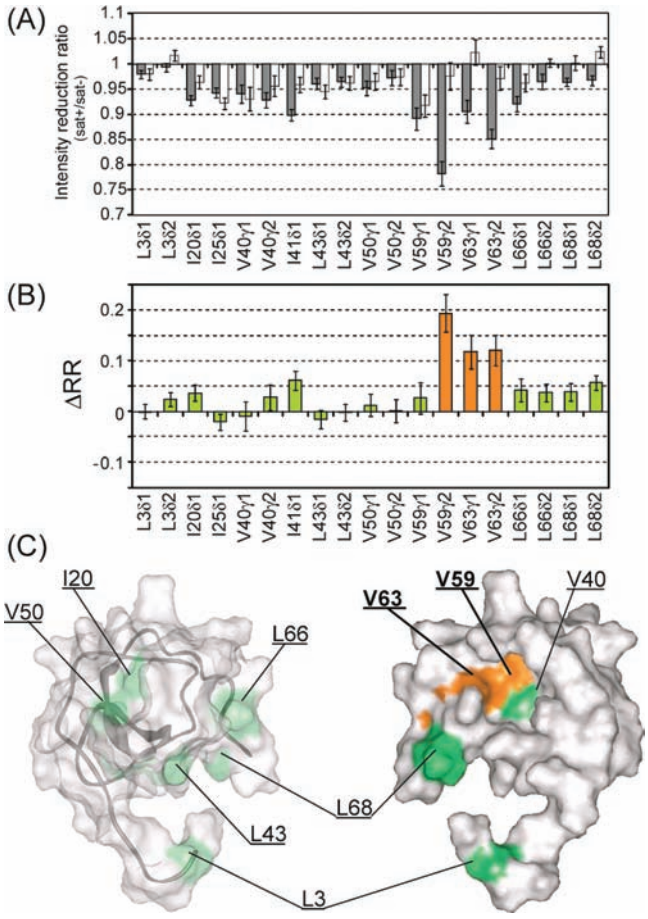

Figure 7. Determination of the CCR5 binding interface on MIP-1α by the methyl-TCS experiments. (A) Plots of the reduction ratios of the signal intensities originating from the isoleucine, leucine, and valine methyl resonances, with and without irradiation. Gray bars represent the ratios from the methyl-TCS experiment with CCR5−rHDL. White bars represent the ratios from the negative control experiment with empty rHDL. The error bars in both graphs represent the experimental errors, calculated from the root sum square of (noise level/signal intensity) in the two spectra, with and without irradiation. (B) Plot of the difference in the reduction ratio (ΔRR). Cross-peaks with ΔRR > 0.1 and <0.1 are colored orange and green, respectively. (C) Mapping of the affected residues in the TCS experiment with CCR5−rHDL on the MIP-1α structure (PDB code: 1B53). These molecular diagrams were generated with WebLab Viewer Pro (Molecular Simulations, Inc.) The Ile, Leu, and Val residues with ΔRR > 0.1 and <0.1 are colored orange and green, respectively.

relative to the cross-saturation between CCR5−rHDL and the MIP-1α variant, due to the short fast internal motions of the methyl protons and the high deuteration level of MIP-1α variant, respectively.[21]

Therefore, we conclude that V59 and V63, with ΔRRs of more than 0.1, are in close proximity to CCR5 in the complex.

Discussion

In the present study, CCR5 was heterologously expressed in insect cells. There are four tyrosine residues to be sulfated in the N-terminus of CCR5, and these N-terminal sulfations reportedly play an important role in the high affinity ligand binding.[64−66] Nisius et al. demonstrated that CCR5 expressed in insect cells is reportedly sulfated.[67] However, the experiment by Nisius et al. cannot determine whether the four potential sulfation sites are completely modified.[68] The EC_{50} for the GDP−GTP exchange assay in the present study (∼100 nM) was significantly larger than those previously reported, using CCR5 expressed in mammalian cells (about a few nanomolar).[8,69,70] The difference in the EC_{50} value may be due to the insufficient tyrosine sulfation of CCR5 expressed in insect cells. Another possible reason for the difference in the EC_{50} value is the absence of the glycosaminoglycans on the CCR5−rHDL.[71−73] However, the ligand binding mode of CCR5 prepared by the method established here is biologically relevant, because the induction of the GDP−GTP exchange of the Gα subunit by CCR5−rHDL and MIP-1β could be observed (Figure 5B). In addition, CCR5 on the cells lacking glycosaminoglycans[71] and the CCR5 mutants (Y3A, Y10A or Δ2−5), which are partially depleted of the sulfation, also exhibited its signaling activity.[74]

Structural analyses of CCR5 have been hampered by its low stability in detergent micelles (Figure 1), although the sample preparation methods aimed toward structural analyses were reported by several groups.[48,50,67,75] Therefore, we tried to

(64) Bannert, N.; Craig, S.; Farzan, M.; Sogah, D.; Santo, N. V.; Choe, H.; Sodroski, J. *J. Exp. Med.* **2001**, *194*, 1661–73.
(65) Farzan, M.; Mirzabekov, T.; Kolchinsky, P.; Wyatt, R.; Cayabyab, M.; Gerard, N. P.; Gerard, C.; Sodroski, J.; Choe, H. *Cell* **1999**, *96*, 667–76.
(66) Duma, L.; Haussinger, D.; Rogowski, M.; Lusso, P.; Grzesiek, S. *J. Mol. Biol.* **2007**, *365*, 1063–75.
(67) Nisius, L.; Rogowski, M.; Vangelista, L.; Grzesiek, S. *Protein Expression Purif.* **2008**, *61*, 155–62.
(68) Seibert, C.; Sakmar, T. P. *Biopolymers* **2008**, *90*, 459–77.
(69) Laurence, J. S.; Blanpain, C.; Burgner, J. W.; Parmentier, M.; LiWang, P. J. *Biochemistry* **2000**, *39*, 3401–9.
(70) Springael, J. Y.; de Poorter, C.; Deupi, X.; Van Durme, J.; Pardo, L.; Parmentier, M. *Cell. Signalling* **2007**, *19*, 1446–56.
(71) Ali, S.; Palmer, A. C.; Banerjee, B.; Fritchley, S. J.; Kirby, J. A. *J. Biol. Chem.* **2000**, *275*, 11721–7.
(72) Proudfoot, A. E. *Biochem. Soc. Trans.* **2006**, *34*, 422–6.
(73) Lortat-Jacob, H. *Curr. Opin. Struct. Biol.* **2009**, *19*, 543–8.
(74) Blanpain, C.; Doranz, B. J.; Vakili, J.; Rucker, J.; Govaerts, C.; Baik, S. S.; Lorthioir, O.; Migeotte, I.; Libert, F.; Baleux, F.; Vassart, G.; Doms, R. W.; Parmentier, M. *J. Biol. Chem.* **1999**, *274*, 34719–27.
(75) Ren, H.; Yu, D.; Ge, B.; Cook, B.; Xu, Z.; Zhang, S. *PLoS One* **2009**, *4*, e4509.

reconstitute CCR5 into lipid bilayer by using rHDL, which is promising for solution NMR studies, because of its water solubility and monodisperse character. Several methods were reported for the preparation of rHDL containing membrane proteins. A kit combining the usage of rHDL and in vitro translation of membrane proteins has recently become commercially available.[26,76] In the most widely used method, the membrane proteins were initially purified in the detergent-solubilized state, and were subsequently reconstituted into rHDL.[77−80] In a different method, P450 solubilized from Sf9 cells was directly incorporated into rHDL, and was subsequently purified by the Ni-affinity and size exclusion chromatographies.[81] In the present study, we employed the third method, among the three methods mentioned above, with modifications such as the purification of the membrane fraction by UC and addition of a 1D4 affinity chromatography step in order to extensively remove the impurities from the cell extract. With this method, we successfully obtained biologically functional CCR5−rHDL.

Considering the extreme instability of solubilized CCR5, it is suitable to reconstitute CCR5 directly from the lysate of Sf9 cells before purification, because the method employed in the present study enables us to minimize the period during which CCR5 is in the solubilized state to ~90 min. Although there are several methodologies for the reconstitution of membrane proteins into lipid bilayers such as proteoliposomes, only rHDL enables reconstitution to be performed prior to purification.[81] In addition, CCR5 reconstituted into rHDL is surrounded by lipids with almost the same composition as that in the cells that express CCR5,[81] because the lipids from the cell membrane were utilized for the rHDL reconstitution (Figure 2). This would also be useful for retaining the function and enhancing the stability of CCR5, because the phospholipid environment is reportedly responsible for coupling activity with G-protein in a GPCR.[82]

The TCS experiment revealed that the region around V59 and V63 of the MIP-1α variant is in close proximity to CCR5 (Figure 7). The CCR5 binding mode of the monomeric MIP-1α variant is biologically relevant, because the induction of the GDP−GTP exchange of the Gα subunit by CCR5−rHDL and monomeric MIP-1α variant could be observed (Supporting Information Figure S4). The secondary structural elements within the MIP-1α variant are similar to those of wild-type MIP-1α from $^{1}H-^{15}N$ HSQC spectrum (Supporting Information Figure S2) and the $^{13}C_{\alpha}$ and $^{13}C_{\beta}$ chemical shifts. In addition, the $^{13}C_{\alpha}$ and $^{13}C_{\beta}$ chemical shifts of the CCR5-binding residues in the MIP-1α variant were almost identical to those of wild-type MIP-1α ($\Delta^{13}C_{\alpha} > 0.7$ ppm, $\Delta^{13}C_{\beta} > 0.4$ ppm for V40, V59, and V63), suggesting that the structural integrity of this region is retained in the MIP-1α variant.

Previous structure−function studies suggested that the N-terminal and N-loop residues on the chemokines are involved in the receptor interaction.[4,9] On the other hand, the region around V63, which forms a hydrophobic cleft, located on the nearly opposite side against the N-terminus and N-loop. This region was not investigated in previous mutational studies of CCR5 ligands, probably because mutating to the hydrophobic residues is difficult.[58] Although the methyl-directed TCS experiments cannot investigate the sites lacking leucine and valine residues, it will be a powerful tool for detecting the binding sites of the molecules, for which a mutational analysis is not suitable.

Several single nucleotide polymorphisms (SNPs) with non-synonymous amino acid change were recently identified within the MIP-1α gene,[83] and one of the SNPs, with substitution of E57, reportedly has a protective genetic influence on HIV-1 infection. However, it was unknown how these SNPs have effects on the MIP-1α function. The present TCS study suggests the possibility that the protective influence on HIV-1 infection of the SNP is due to the change of the interaction mode between CCR5 and MIP-1α, which causes the increased affinity, because E57 is in close proximity to V59 and V63. In addition, another SNP contains substitution of V63 itself.[84] Although this SNP has not been well characterized, this SNP may also have a genetic influence on HIV-1 infection.

Classically, GPCRs including chemokine receptors have been considered to function as monomers.[85] β_2AR and rhodopsin reconstituted into rHDL as monomers reportedly activated G proteins.[79,86] It is likely that CCR5 exists as a monomer in rHDL in the present study, considering the molar ratio of CCR5 and MSP in the preparation steps.[78]

Increasing evidence has suggested that GPCRs exist as homodimers or heterodimers on the cell surface, which are thought to engage in an additional mechanism for modulating the receptor function.[85,87−90] Further studies are necessary for clarification, and the methods we have established here, along with the previously reported method for preparing rHDL with receptor oligomer,[78,91−93] may be helpful for investigating the chemokine receptor multimerization.

In this report, we have established a method for the structural analyses of the interactions between CCR5 and its ligand MIP-1α, although CCR5 is extremely labile in the detergent-solubilized state. Our refined rHDL reconstitution method along with the methyl-TCS experiments will facilitate structural analyses of membrane proteins with low yield and low stability,

(76) Cappuccio, J. A.; et al. *Methods Mol. Biol.* **2009**, *498*, 273–96.
(77) Leitz, A. J.; Bayburt, T. H.; Barnakov, A. N.; Springer, B. A.; Sligar, S. G. *BioTechniques* **2006**, *40*, 601−2, 604, 606, passim.
(78) Bayburt, T. H.; Leitz, A. J.; Xie, G.; Oprian, D. D.; Sligar, S. G. *J. Biol. Chem.* **2007**, *282*, 14875–81.
(79) Whorton, M. R.; Bokoch, M. P.; Rasmussen, S. G.; Huang, B.; Zare, R. N.; Kobilka, B.; Sunahara, R. K. *Proc. Natl. Acad. Sci. U.S.A.* **2007**, *104*, 7682–7.
(80) Kuszak, A. J.; Pitchiaya, S.; Anand, J. P.; Mosberg, H. I.; Walter, N. G.; Sunahara, R. K. *J. Biol. Chem.* **2009**, *284*, 26732–41.
(81) Civjan, N. R.; Bayburt, T. H.; Schuler, M. A.; Sligar, S. G. *BioTechniques* **2003**, *35*, 556−60, 562−3.
(82) Jastrzebska, B.; Goc, A.; Golczak, M.; Palczewski, K. *Biochemistry* **2009**, *48*, 5159–70.
(83) Modi, W. S.; Lautenberger, J.; An, P.; Scott, K.; Goedert, J. J.; Kirk, G. D.; Buchbinder, S.; Phair, J.; Donfield, S.; O'Brien, S. J.; Winkler, C. *Am. J. Hum. Genet.* **2006**, *79*, 120–8.
(84) Paximadis, M.; Mohanlal, N.; Gray, G. E.; Kuhn, L.; Tiemessen, C. T. *Int. J. Immunogenet.* **2009**, *36*, 21–32.
(85) Salanga, C. L.; O'Hayre, M.; Handel, T. *Cell. Mol. Life Sci.* **2009**, *66*, 1370–86.
(86) Whorton, M. R.; Jastrzebska, B.; Park, P. S.; Fotiadis, D.; Engel, A.; Palczewski, K.; Sunahara, R. K. *J. Biol. Chem.* **2008**, *283*, 4387–94.
(87) Milligan, G.; Smith, N. J. *Trends Pharmacol. Sci.* **2007**, *28*, 615–20.
(88) El-Asmar, L.; Springael, J. Y.; Ballet, S.; Andrieu, E. U.; Vassart, G.; Parmentier, M. *Mol. Pharmacol.* **2005**, *67*, 460–9.
(89) Issafras, H.; Angers, S.; Bulenger, S.; Blanpain, C.; Parmentier, M.; Labbe-Jullie, C.; Bouvier, M.; Marullo, S. *J. Biol. Chem.* **2002**, *277*, 34666–73.
(90) Mellado, M.; Rodriguez-Frade, J. M.; Vila-Coro, A. J.; Fernandez, S.; Martin de Ana, A.; Jones, D. R.; Toran, J. L.; Martinez, A. C. *EMBO J.* **2001**, *20*, 2497–507.
(91) Banerjee, S.; Huber, T.; Sakmar, T. P. *J. Mol. Biol.* **2008**, *377*, 1067–81.
(92) Bayburt, T. H.; Grinkova, Y. V.; Sligar, S. G. *Arch. Biochem. Biophys.* **2006**, *450*, 215–22.
(93) Boldog, T.; Li, M.; Hazelbauer, G. L. *Methods Enzymol.* **2007**, *423*, 317–35.

by placing them in a lipid bilayer environment to retain their biological functions. This method will be applicable to the various and complicated networks of interactions in GPCR signaling, such as lipids, ligands, G-proteins, and other effector molecules.

Acknowledgment. We thank Dr. Haruko Hayasaka for her helpful advice. This work was supported by a grant from the Japan New Energy and Industrial Technology Development Organization (NEDO).

Supporting Information Available: SEC analysis of empty rHDL, NMR spectra of the MIP-1α variant, GDP−GTP exchange assay with the MIP-1α variant, the control TCS experiment with the 2D7-antibody, and complete refs 58 and 76. This material is available free of charge via the Internet at http://pubs.acs.org.

JA100830F